

# Ultranarrow coupling-induced transparency bands in hybrid plasmonic systems

Thomas Zentgraf,<sup>1,2</sup> Shuang Zhang,<sup>1</sup> Rupert F. Oulton,<sup>1</sup> and Xiang Zhang<sup>1,3</sup>

<sup>1</sup>NSF Nano-scale Science and Engineering Center, University of California, 3112 Etcheverry Hall, Berkeley, California 94720, USA

<sup>2</sup>Physikalisches Institut, Universität Stuttgart, Pfaffenwaldring 57, 70550 Stuttgart, Germany

<sup>3</sup>Material Sciences Division, Lawrence Berkeley National Laboratory, Berkeley, California 94720, USA

(Received 26 July 2009; published 18 November 2009)

Plasmons in nanoscale structures represent an exciting new route toward efficient manipulation of photons, especially at subwavelength scales. Of particular interest are the hybridized plasmonic systems, in which the interaction among the plasmonic elements can be utilized to tailor the optical responses. Here we demonstrate a hybridized plasmonic-waveguide system exhibiting behavior similar to that of the electromagnetically induced transparency; namely, an ultranarrow transmission line width arising from a coupling-induced cancellation of the plasmonic resonance.

DOI: 10.1103/PhysRevB.80.195415

PACS number(s): 78.20.Ci, 42.50.Gy, 73.20.Mf, 78.67.-n

## I. INTRODUCTION

Much of the richness and variety of physics today is based on coupling phenomena where multiple interacting systems hybridize into new ones with completely distinct attributes. Nordlander and co-workers<sup>1</sup> first proposed the concept of plasmonic hybridization by finding a connection between coupled plasmonic ensembles and the electronic orbitals of atomic molecules. As shown by a number of recent works, well-designed hybridized plasmonic systems can offer exotic optical properties that cannot be readily achieved with natural materials. Good examples are the double metallic rods that provide negative magnetic responses<sup>2,3</sup> and coupled radiative-dark artificial plasmonic “molecules” for constructing all-optical electromagnetic-induced transparency (EIT) metamaterials.<sup>4</sup> However, due to the metal loss, the performances of many plasmonic systems are considerably limited. One way around this issue is to mediate the coupling by a cavity or dielectric waveguide.<sup>5-7</sup> The coherent interaction between a waveguide mode and a plasmonic mode can be utilized to engineer the resonant features of the hybridized system, such as the resonant frequencies, the line width and line shape.<sup>8-11</sup> Here, we show that a waveguide coherently coupled to periodic plasmonic resonators can exhibit extremely narrow transmission peaks in the spectrum as well as a strong dispersion and a significantly reduced group velocity. These findings are quite unexpected considering the large material loss of metal at optical wavelengths. Such EIT-like behavior is of practical significance for applications ranging from sensing to optical communications and optical nonlinearity enhancement at short propagation distances.<sup>12</sup>

## II. HYBRID PLASMONIC WAVEGUIDE SYSTEM

The proposed structure consists of periodic gold nanowires embedded in a high dielectric permittivity slab waveguide on top of a lower dielectric index substrate. An illustration of the entire structure as well its profile are shown in Figs. 1(a) and 1(b), respectively. The incoming electromagnetic wave, propagating in the normal ( $-z$ ) direction with electric field polarization in the  $x$  direction, can excite localized surface-plasmon polaritons (LSPPs) in each metal wire, leading to a broadband strong absorption and scattering peak

in the spectrum. The periodic arrangement of the metal nanowires provides the necessary momentum to couple the coherent scattering of the plasmonic resonances into the transversal magnetic (TM) waveguide mode. Consequently, this system can be described as a coupled system of orthogonal radiation and guided modes, which is mediated by the plasmonic resonance of the metal nanowires. For a given thickness  $t$  of the waveguide, the period  $d$  determines the frequency at which the incident light and guided mode couple<sup>13</sup> while the LSPP resonance frequency is given by the geometrical size (cross section) of the wires and the permittivities of the surrounding media.<sup>14</sup> In our analysis the nanowires have a cross section of  $100 \times 15 \text{ nm}^2$  and are made of gold. For the permittivity of gold the values from Ref. 15 were taken into account. The wires are embedded in a waveguide material with  $\epsilon_{\text{wg}}=3.8$  on top of a quartz substrate ( $\epsilon=2.4$ ). All spectra are calculated by utilizing a rigorous coupled wave analysis (RCWA), which expands the electromagnetic field into 301 diffraction orders and matches the boundary conditions at each interface.<sup>16</sup> For all calculations we assume an infinite grating in  $x$  direction. However, finite

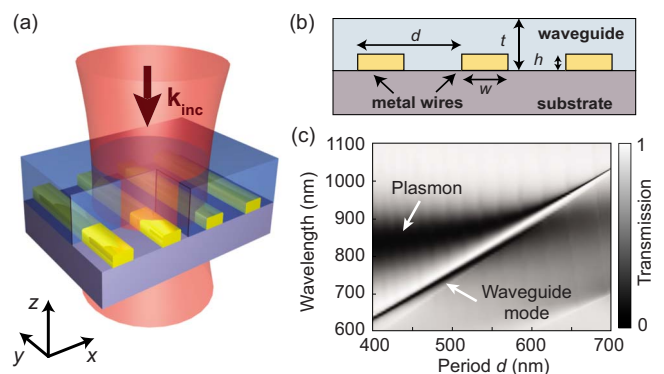


FIG. 1. (Color online) (a) Illustration of the hybrid structure with light propagation in negative  $z$  direction and field polarization in  $x$  direction. (b) Structure cross section together with the geometrical parameters. (c) Calculated transmission in dependence on the nanowire period  $d$  for a 200-nm-thick waveguide ( $\epsilon_{\text{wg}}=3.8$ ). The strong scattering and absorption of the Plasmons and the excitation of the waveguide mode lead to low transmission (dark color). For periods around 580 nm the hybrid-plasmon-waveguide modes are separated by a narrow high-transmission band.

gratings or a nonperfect periodicity will result in a momentum distribution due to the broadening of the grating vector and subsequently lead to a broader waveguide resonance.<sup>11,17</sup> Hence, the coherent scattering of the plasmonic resonances into a specific waveguide mode is reduced and coupling becomes weaker.

The coupling between the LSPPs and the waveguide mode results in a waveguide-plasmon hybridization with distinct properties for the transmission.<sup>18</sup> By changing the spectral mode position of the original waveguide resonance with respect to the LSPP resonances leads to a pronounced anticrossing of the dispersion bands as shown in Fig. 1(c). Although the position of the hybridized modes depends on the angle of incidence for the light,<sup>13</sup> we will focus first on the normal incidence to the surface. In the case the bare modes (TM waveguide mode and LSPPs) spectrally overlap a narrow transmission band is formed within the broad absorption and scattering band of the LSPPs. This transmission band can be observed in Fig. 1(c) for a wire period of  $d \approx 600$  nm. However, the width of this transmission band is determined by the coupling strength between the bare modes. It arises from the destructive interference between the two excitation pathways, namely, the direct excitation of LSPPs in the metal wires and the excitation of the waveguide mode through the scattering of the LSPPs of metal wires as well as the back coupling to them. The anticrossing of the new-coupled eigenmodes in Fig. 1(c) with a pronounced high transmission band cannot be obtained by a simple periodic arrangement of nanowires on a dielectric surface without a waveguide resonance. However, the direct radiative coupling between the localized plasmon modes in the nanowires can be drastically enhanced with a grating anomaly, resulting in a strong spectral lineshape change in the plasmon resonance. Detailed discussions of this additional effect can be found in Refs. 13 and 19.

Since the transmission band is directly related to the appearance of the TM waveguide mode, its spectral position can be roughly estimated by solving the dispersion relation of the TM slab mode<sup>20</sup> for the given momentum of the nanowire grating  $G=2\pi/d$ . If the TM mode spectrally overlaps with the LSPP resonance the coupling-induced transmission band will appear approximately at the original waveguide mode position.

### III. RESULTS AND DISCUSSION

#### A. Ultranarrow transparency bands

For applications such as slow light and sensing, a narrow EIT-like transparency window is highly desirable. In the following we show how extremely narrow transmission peaks within the broad plasmonic resonance can be obtained by reducing the coupling between the plasmonic and waveguide modes. The coupling is extremely sensitive to the value of a single parameter—the thickness of the waveguide. This is depicted in Fig. 2(a), where the reduction in the thickness  $t$  of the dielectric waveguide from 180 to 130 nm dramatically decreases the width of the transmission band between the two hybrid modes that are formed by the underlying coupling mechanism mentioned before. Meanwhile, the trans-

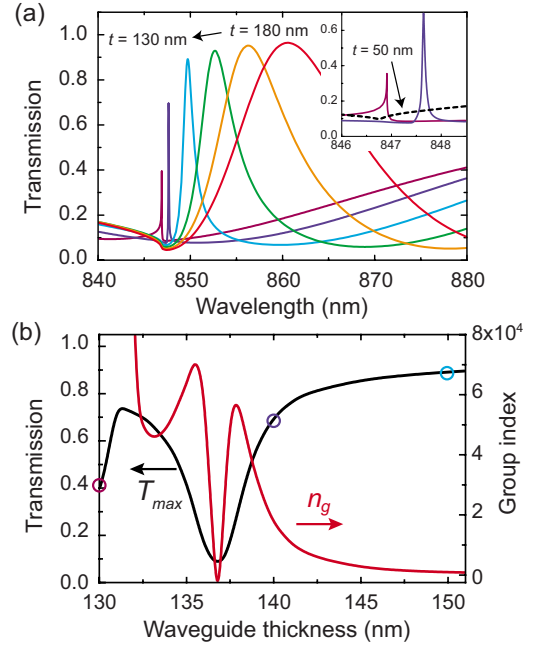


FIG. 2. (Color online) (a) Narrowing of the transmission band in dependence on the waveguide thickness  $t$ . The thickness is changed in steps of 10 nm. The inset shows a magnified view for  $t=130$  and 140 nm together with 50 nm waveguide thickness (black dotted line), which is well below the cutoff for the TM mode. Only a kink due to the Rayleigh anomaly is observable. (b) Maximum transmission value  $T_{max}$  of the transmission band for  $t$  close to the cut-off thickness and the corresponding group index  $n_g$ . The circles mark the transmission for the three smallest thicknesses from panel (a). All calculations are done for  $d=580$  nm.

parency peak shifts to shorter wavelength due to the dependence of the dielectric waveguide mode on its thickness. Further studies show that equally narrow transmission bands can be achieved for even slightly rounded nonrectangular cross sections of the nanowires. Apparently, the transmission window becomes extremely narrow when the waveguide thickness approaches  $t=130$  nm and is accompanied by a reduction in the transmission itself. At that point the dispersion relation of the waveguide mode and the Rayleigh anomaly are identical, resulting in a strong increased coupling by the opening of a new diffraction order. However, the coupling with the Rayleigh anomaly leads to an extinction peak<sup>21</sup> instead of high transmission. This is illustrated in the inset of Fig. 2(a), where no transmission peak is observable for a waveguide thickness of  $t=50$  nm but a kink at  $\lambda \approx 846.7$  nm due to the Rayleigh anomaly. For the chosen set of parameters the waveguide mode reaches the cutoff at  $t \approx 132$  nm. The sharp transmission peak is associated with a dramatic change in the transmission phase (refractive index), consequently, extremely slow group velocity of light traversing the system can be achieved. Figure 2(b) shows a more detailed analysis of the transmission close to the cut-off thickness. A decrease below 10% can be observed for a thickness of  $t=137$  nm. For slightly smaller values of  $t$  the transmission increases again up to nearly 80%. Figure 2(b) shows the corresponding group index  $n_g$  for the transmission band. The group index increases with decreasing thickness of

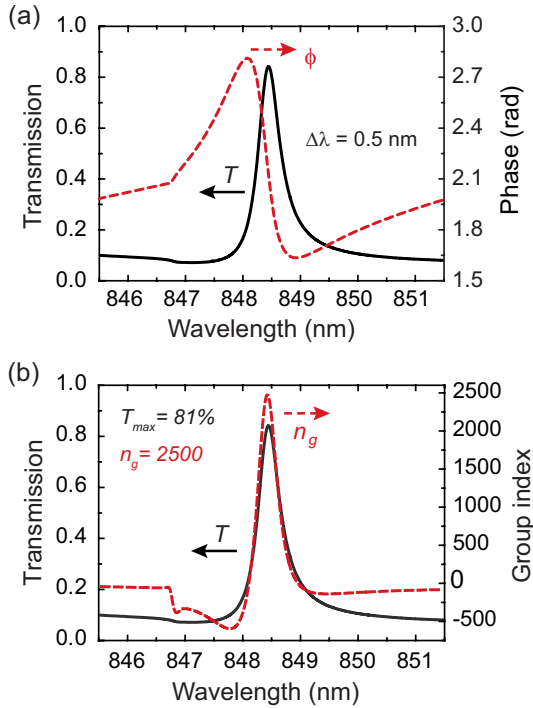


FIG. 3. (Color online) (a) Calculated transmission (straight black line) and phase (dotted red line) for a structure with a wire period of  $d=580$  nm and a waveguide thickness of  $t=145$  nm. The resulting group index for these parameters is shown in (b) together with the transmission.

the waveguide except for the range around 137 nm where the group index suddenly drops 4 orders of magnitude.

For a detailed analysis of this behavior, we fix the thickness of the waveguide slab to  $t=145$  nm, where a reasonably sharp peak and a transmission of more than 80% are obtained. Figure 3(a) shows the calculated transmission and the phase change for this configuration. The transmission peak has a full width half maximum of  $\Delta\lambda=0.5$  nm within a broadband low-transmission region of the plasmonic resonances and is accompanied by a phase change of nearly  $\pi/2$ . The group index  $n_g$  is calculated from the dispersion of the phase  $\phi$  by

$$n_g = c_0 \frac{dk}{d\omega} = \frac{c_0}{t} \frac{d\phi}{d\omega}. \quad (1)$$

Here,  $c_0$  is the speed of light in vacuum and  $\omega$  is the angular frequency. The dependence of the transmission and the group index on wavelength is plotted in Fig. 3(b). The strong dispersion of the phase results in a group index of  $n_g \approx 2500$  at the maximum of the transmission band. The high group index corresponds to an increased traversing time of light through the entire structure. In plasmonic structures the absorption of the metal would normally lead to strong energy dissipation and a distinct reduction in the transmission if the light would be stored for a long time in the plasmonic resonators. However, the plasmonic field of the nanowires is canceled out due to the unique form of the coupling to the waveguide mode whereas the degree of cancellation is related to interference between radiation and quasiguided modes. This

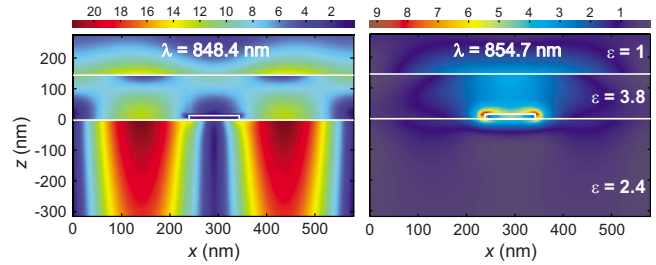


FIG. 4. (Color online) Magnitude of the total electric field for two different wavelengths normalized to the input field. The solid lines at  $z=0$  and 145 nm denote the interfaces of the waveguide and the cross section of the metal wires. The left panel shows the field at the maximum of transmission at  $\lambda=848.4$  nm where the field avoids the region of the metal wires. The right panel is for a slightly longer wavelength of 854.7 nm where the transmission has a minimum due to the strong interaction of the light with the Plasmon resonance.

cancellation results in weak local fields near the metal and therefore low absorption between the two branches of the hybrid modes. Figure 4 illustrates the local electric field distribution in the structure at two different wavelengths. At the wavelength of the transmission peak ( $\lambda=848.4$  nm) the fields are strongly localized in the dielectric areas, especially at the waveguide-substrate interface in the space between the gold nanowires. The field distribution along the  $z$  axis is characteristic of a guided TM slab mode. Directly at the nanowires the field is suppressed due to the aforementioned destructive interference between the two excitation pathways. The scenario changes completely for a slight shift of the wavelength to 854.7 nm (minimum of the transmission), where the field is mainly localized around the nanowire, a typical sign for the strong excitation of the LSPP.

**B. Coupling mechanisms**

As shown in Fig. 2(a), the transmission peak becomes extremely narrow when the thickness of the dielectric waveguide slab is reduced. This effect can be understood in the modified coupling of the LSPP to the waveguide mode. To gain more insight we perform a calculation of the electric field distribution of an unperturbed TM waveguide mode for a dielectric slab without grating. The total electric field consists of two components ( $E_x$  and  $E_z$ ) whereas only the weaker  $E_x$  component can couple to the resonant-charge oscillation of the LSPP mode of the metal wires in  $x$  direction. The LSPP resonance of the nanowires in  $z$  direction appears at much shorter wavelengths and will not couple with the TM waveguide mode. Therefore, we focus in the following only on  $E_x$  component.

Figure 5 shows the analytically obtained  $|E_x|$  component of the electric field (solid line) along  $z$  for a TM waveguide eigenmode at  $\lambda=848.4$  nm ( $t=145$  nm) for the case when no plasmonic grating is present inside the waveguide. The field shows a local minimum with zero-field strength inside the slab near the substrate-waveguide interface at  $z=13$  nm. The coupling strength between LSPPs (bright mode) and the waveguide mode (dark mode) depends on the overlap inte-

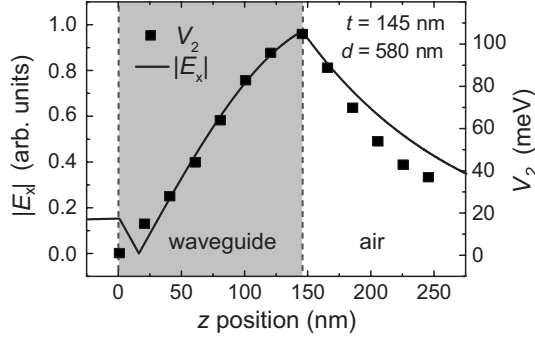


FIG. 5. Magnitude of the electric field component  $E_x$  of the TM slab mode (solid line) for a cross section along the  $z$  axis. The dots are the calculated coupling parameters  $V_2$  between the plasmonic resonances of the grating and the quasiguidded TM mode for different position  $z$  of nanowires.

gral of the  $E_x$  field of the waveguide mode and the Plasmon field, which is strongest in  $x$  direction. Therefore, we expect that the coupling strength will increase by placing the nanowire grating closer to the waveguide-air interface (but inside the slab) because  $|E_x|$  increases with decreasing distance to the air interface. To prove this assumption we utilize an effective Hamiltonian  $H_{\text{eff}}$  near the center of the first Brillouin zone<sup>18</sup>

$$H_{\text{eff}} = \begin{pmatrix} E_{\text{wg}} + \tilde{c}k_x & V_1 & V_2 \\ V_1 & E_{\text{wg}} - \tilde{c}k_x & V_2 \\ V_2 & V_2 & E_{\text{pl}} - i\Gamma \end{pmatrix} \quad (2)$$

whereas  $E_{\text{wg}}$  and  $\tilde{c}$  are the TM mode energy and the group velocity,  $E_{\text{pl}}$  and  $\Gamma$  the energy and the damping of the individual LSPPs,  $V_1$  the photon-photon coupling energy between the symmetric and antisymmetric TM modes, and  $V_2$  the waveguide-plasmon coupling energy. Equation (2) is derived from a set of coupled equations that phenomenologically describe the coupling behavior of the original “bare” modes in the system. Hence, after introducing the coupling constants  $V_N$  between the original modes, the eigenvalues of the effective Hamiltonian represent the new energy eigenstates (or resonance frequencies) of the coupled (hybrid) system. The corresponding eigenfunctions of the Hamiltonian characterize the new noninteracting plasmon-waveguide hybrid modes. In the following, we are interested in the case where the incoming light is propagating in  $z$  direction ( $k_x=0$ ). Extinction spectra are calculated for different  $z$  positions of the nanowire grating inside the waveguide slab. By fitting  $H_{\text{eff}}$  to the numerically obtained spectra, the coupling parameter  $V_2$  can be extracted in dependence on the  $z$  position of the nanowires. The results are plotted in Fig. 5 together with  $|E_x|$  of an unperturbed TM waveguide mode. As the wires have a finite height of 15 nm in  $z$  direction, the position in the plot corresponds to the edge of the nanowires closer to the substrate interface (e.g., the value for  $z=0$  means the grating is placed on the substrate surface and reaches 15 nm into the waveguide). Obviously the coupling parameter  $V_2$  follows the trend of  $|E_x|$  and shows the smallest values near the substrate-waveguide interface.<sup>22</sup>

The eigenvalues of  $H_{\text{eff}}$  correspond to the energies (spectral positions) of the hybridized modes. A justified approximation is that the coupling energy between the waveguide modes is small compared to all other coupling energies ( $V_1 \ll V_2, \Gamma$ ). Hence, the three eigenvalues of the Hamiltonian are  $E_1 = E_0$  and  $E_{2,3} = 0.5[2E_0 - i\Gamma \pm \sqrt{8V_2^2 - \Gamma^2}]$  whereas we assume  $E_0 = E_{\text{wg}} = E_{\text{pl}}$ . Interestingly, the eigenfunction  $\Psi(E_1) = \{\tilde{\Psi}_1, \tilde{\Psi}_2, \tilde{\Psi}_3\}$  exhibits only components of the original bare waveguide mode ( $\tilde{\Psi}_1 = -\tilde{\Psi}_2$ ) but no plasmonic counterpart ( $\tilde{\Psi}_3 = 0$ ). Since the bare waveguide mode was assumed to be lossless, this particular eigenmode of the hybrid system does not suffer from losses in the metal by the excitation of LSPPs and therefore can have a high transmission. This mode corresponds to the electric field distribution shown in Fig. 4 (left panel) with nearly no field around the metal nanowire. However, for extremely weak coupling the loss of the waveguide mode (dark mode) has to be taken into account since it will limit the attainable band width and maximum transmission value. Although the dielectric waveguide is nearly loss less, the metal nanowires will introduce absorption loss for the  $E_z$  component of the waveguide mode despite a weak coupling of the  $E_x$  field.

If the field component  $E_x$  of the bare waveguide mode goes to zero the coupling between the waveguide mode and the LSPP vanishes ( $V_2=0$ ) and the eigenvalues of  $H_{\text{eff}}$  degenerate. As a result, the transmission band disappears and the group index  $n_g$  is strongly reduced. This behavior can be observed in Fig. 2(b) for a waveguide thickness of 137 nm, where the  $E_x$  component of the TM mode averages to zero for the nanowire cross section. Therefore, a coupling is not possible and the system is dominated by the response of the LSPPs. A slight decrease or increase in the waveguide thickness increases  $V_2$  and lifts the degeneracy of the eigenmodes, resulting in the transmission band and large values of  $n_g$ .

### C. Symmetric waveguide environment

For an asymmetric waveguide with air on one side and a substrate on the other side the electric field inside the waveguide shows a strong asymmetry with smaller  $|E_x|$  components closer to the substrate interface. With the assumption that the plasmonic nanowires are placed at the substrate side the narrowest transmission peak can be obtained for a waveguide thickness close to the cutoff (Fig. 2). Since the dispersion relation of the waveguide mode and the diffraction anomaly (Rayleigh anomaly) match at that point a clear separation of both effects is difficult. Furthermore, the Rayleigh anomaly can lead to a direct strong dipolar interaction between the LSPPs leading to strong broadening and shift in the spectrum of the Plasmon resonances.<sup>19</sup>

However, in a symmetric configuration for the waveguide with the same material on both sides,  $|E_x|$  becomes symmetric and, more important, the cutoff for the waveguide modes vanishes. As a result the dispersion relation for the waveguide mode and the diffraction anomaly can be distinguished. Figure 6 shows the mode positions for a symmetric waveguide structure ( $t=145$  nm,  $\epsilon_{\text{wg}}=3.8$ , and  $\epsilon_{\text{sur}}=2.4$ ). The nanowires were placed inside the waveguide 5 nm away from the center.

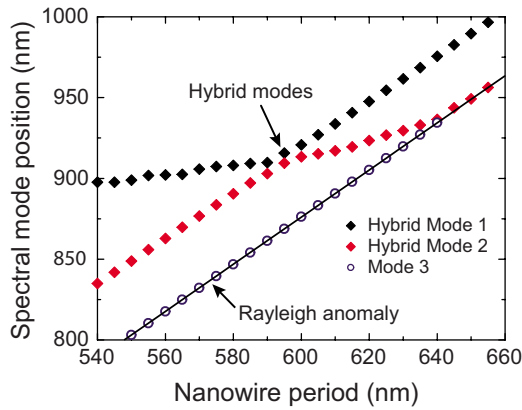


FIG. 6. (Color online) Band diagram showing the positions of the modes obtained from the RCWA calculation for different nanowire periods. The anticrossing of the hybrid modes (black and red squares) is clearly separated from the Rayleigh anomaly (blue circles). The black line is the analytical calculation for the Rayleigh anomaly based on the refractive index.

In this configuration the Rayleigh anomaly is clearly separated from the waveguide dispersion. Nevertheless, the small anticrossing between the hybrid modes and the formation of the narrow transmission band can be observed for a wire period of  $d \approx 590$  nm. Since  $|E_x|$  is symmetric with respect to the center of the waveguide the weakest coupling between the nanowires and the waveguide mode is observed for wires in the middle of the waveguide. This fact is illustrated in Fig. 7 where the magnitude of electric field component  $|E_x|$  is plotted together with the coupling constant  $V_2$  between the nanowire plasmons and the quasiguided TM mode for different positions of the wires. Although the spatial behavior of  $|E_x|$  has changed completely compared to the asymmetric case, the coupling constant follows the trend of  $|E_x|$  with smallest values in the center of the waveguide. Therefore, a narrow transmission band can be obtained for nanowires placed close to the center of the waveguide (e.g., see Fig. 8).

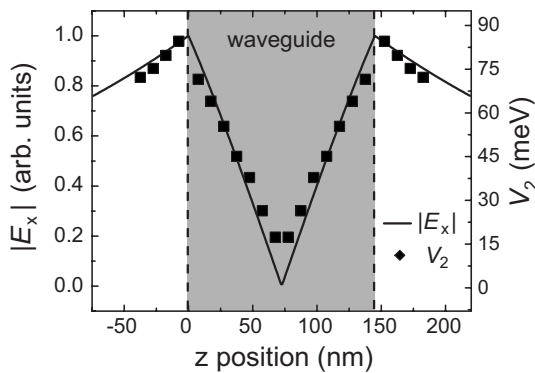


FIG. 7. Magnitude of the electric field component  $E_x$  of the TM slab mode (black solid line) for a cross section along the  $z$  axis. The waveguide has the same environment at both sides resulting in a symmetric magnitude for the field. The dots correspond to the calculated coupling parameters  $V_2$  between the plasmonic resonances of the grating and the quasiguided TM mode for different position  $z$  of wires within the waveguide slab. The period is 580 nm and the thickness of the waveguide is 145 nm (gray shaded area).

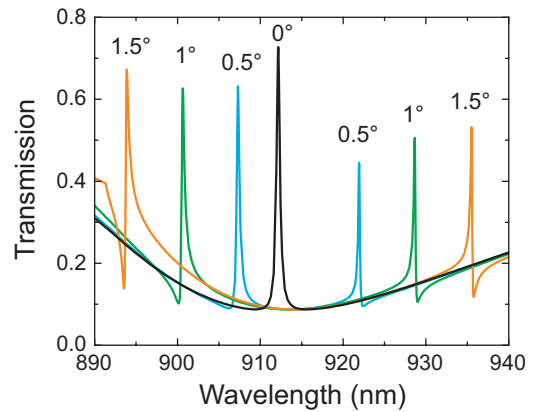


FIG. 8. (Color online) Angular dependence of the transmission band. Shown is the spectral region of the transmission peak for four different angles. Except for the normal incidence two transmission bands appear due to the excitation of the symmetric and the anti-symmetric waveguide mode. The period is 595 nm and the thickness of the waveguide is 145 nm. The nanowires are placed 5 nm away from the center of the symmetric waveguide.

The dependence of the group index and the transmission bandwidth on the nanowire position  $z$  is therefore similar to Fig. 2(b). Hence, the coupling and the transmission band vanish completely for a position directly at the center.

Taking this into account the coupling strength and therefore the spectral width of the transmission band can be engineered by changing the position of the grating or the thickness of the waveguide. We note that different geometries for the plasmonic structures (instead of nanowires) can provide even higher values for the group index but would lead to smaller changes in the absolute transmission. Strictly speaking, the bandwidth of the transmission peak is determined by the coupling constant between the modes. However, the peak value of the transmission is limited by the total loss of the quasiguided TM mode (dark mode) which includes the absorption losses introduced by the metal nanowires. Therefore, a sufficient large coupling is needed for remaining high values of the group index.<sup>4</sup>

#### D. Angular dependence

For practical applications the angular dependence of the transmission band plays an important role. Like other periodic structures the spectral response of the plasmonic hybrid system changes for different angles of incidence. This becomes obvious from Eq. (2) where the eigenvalues of the Hamiltonian depend on  $k_x$ . In the case  $k_x \neq 0$  the degeneracy between the symmetric and the anti-symmetric quasiguided TM mode will be lifted and two waveguide modes couple to the plasmonic resonance of the nanowires. Hence, two transmission band regions will appear whereas the spectral position depends on the angle of incidence. Figure 8 shows the transmission band region for various angles of incidence. The transmission peaks due to the symmetric and the anti-symmetric modes appear on the left and right side of the original peak ( $0^\circ$ ), respectively. The band width is nearly preserved and only the absolute transmission value is slightly

reduced. However, for best performance the waveguide mode position has to overlap with the plasmonic response of the nanowires which could be achieved by modifying the period of the lattice.

### E. Application for refractive-index sensing

Narrow transmission lines are potentially interesting for sensing application due the high sensitivity of their transmission properties to the refractive index of the surrounding medium. To evaluate the performance of the plasmonic-waveguide hybrid system, we chose the same structure geometry as for the calculation of Fig. 8. The transmission change  $\Delta T$  was calculated for a wavelength of  $\lambda = 912.1$  nm close to the peak transmission of structure as a function of the relative refractive index change  $\Delta n/n$ , whereas  $n = 1.46$  was chosen (Fig. 9). Even for small changes in the refractive index of less than  $10^{-4}$ , noticeable changes in the transmission of around 4% can be obtained. With further optimization of the nanowire position and waveguide thickness the sensitivity for refractive index changes will further increase.

## IV. CONCLUSION

We have shown that coherently coupled LSPs with an optical waveguide mode can support extremely narrow transmission bands together with a very high group index. The bandwidth can be modified by changing the position of nanowires with respect to the waveguide mode. Since the transmission and the group index are highly sensitive to waveguide thickness (i.e., effective index) and nanowire position, the structure could be interesting as a new class of nano-optical sensors. Especially the asymmetric waveguide struc-

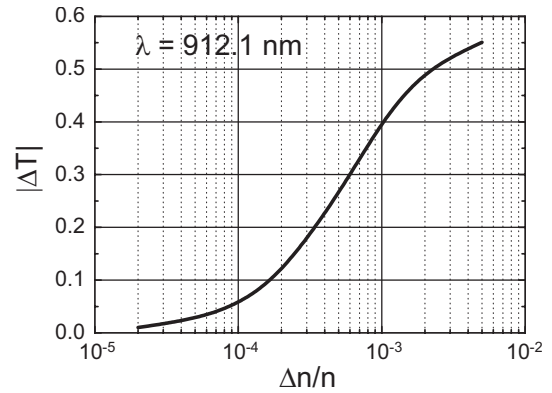


FIG. 9. Change in the transmission in dependence of the relative refractive index change in the surrounding material. The transmission values are calculated for the same structure geometry used in Fig. 8 for the angular dependence. The transmission was calculated for a wavelength of  $\lambda = 912.1$  nm close to the peak transmission of the structure in dependence on the refractive index of the surrounding top-half space.

ture is easy to fabricate, it could be an interesting candidate for slowing down light and enhancing nonlinear effects for integrated nano-optic devices without using materials with large nonlinear coefficients.

## ACKNOWLEDGMENTS

We thank Guy Bartal and Atsushi Ishikawa for stimulating discussion and acknowledge financial support from the U.S. Department of Energy under Contract No. DE-AC02-05CH11231. T.Z. thanks the Alexander von Humboldt Foundation and the Landesstiftung Baden-Württemberg for their support.

- <sup>1</sup>E. Prodan, C. Radloff, N. J. Halas, and P. Nordlander, *Science* **302**, 419 (2003).
- <sup>2</sup>V. M. Shalaev, W. Cai, U. K. Chettiar, H.-K. Yuan, A. K. Sarychev, V. P. Drachev, and A. V. Kildishev, *Opt. Lett.* **30**, 3356 (2005).
- <sup>3</sup>N. Liu, H. Guo, L. Fu, S. Kaiser, H. Schweizer, and H. Giessen, *Adv. Mater. (Weinheim, Ger.)* **19**, 3628 (2007).
- <sup>4</sup>S. Zhang, D. A. Genov, Y. Wang, M. Liu, and X. Zhang, *Phys. Rev. Lett.* **101**, 047401 (2008).
- <sup>5</sup>S. Linden, J. Kuhl, and H. Giessen, *Phys. Rev. Lett.* **86**, 4688 (2001).
- <sup>6</sup>R. Oulton, V. Sorger, D. A. Genov, D. F. P. Pile, and X. Zhang, *Nat. Photonics* **2**, 496 (2008).
- <sup>7</sup>J. A. Porto, F. J. Garcia-Vidal, and J. B. Pendry, *Phys. Rev. Lett.* **83**, 2845 (1999).
- <sup>8</sup>P. N. Stavrinou and L. Solymar, *Phys. Rev. E* **68**, 066604 (2003).
- <sup>9</sup>T. Zentgraf, A. Christ, J. Kuhl, and H. Giessen, *Phys. Rev. Lett.* **93**, 243901 (2004).
- <sup>10</sup>T. Utikal, T. Zentgraf, J. Kuhl, and H. Giessen, *Phys. Rev. B* **76**, 245107 (2007).
- <sup>11</sup>D. Nau, A. Schönhardt, Ch. Bauer, A. Christ, T. Zentgraf, J. Kuhl, M. W. Klein, and H. Giessen, *Phys. Rev. Lett.* **98**,

133902 (2007).

- <sup>12</sup>R. W. Boyd and D. J. Gauthier, *Nature (London)* **441**, 701 (2006).
- <sup>13</sup>A. Christ, T. Zentgraf, J. Kuhl, S. G. Tikhodeev, N. A. Gippius, and H. Giessen, *Phys. Rev. B* **70**, 125113 (2004).
- <sup>14</sup>U. Kreibig and M. Vollmer, *Optical Properties of Metal Clusters* (Springer, Berlin, 1995).
- <sup>15</sup>P. B. Johnson and R. W. Christy, *Phys. Rev. B* **6**, 4370 (1972).
- <sup>16</sup>M. G. Moharam and T. K. Gaylord, *J. Opt. Soc. Am.* **71**, 811 (1981).
- <sup>17</sup>T. Zentgraf, A. Christ, J. Kuhl, N. A. Gippius, S. G. Tikhodeev, D. Nau, and H. Giessen, *Phys. Rev. B* **73**, 115103 (2006).
- <sup>18</sup>A. Christ, S. G. Tikhodeev, N. A. Gippius, J. Kuhl, and H. Giessen, *Phys. Rev. Lett.* **91**, 183901 (2003).
- <sup>19</sup>B. Lamprecht, G. Schider, R. T. Lechner, H. Ditlbacher, J. R. Krenn, A. Leitner, and F. R. Aussenegg, *Phys. Rev. Lett.* **84**, 4721 (2000).
- <sup>20</sup>K. Kawano and T. Kitho, *Introduction to Optical Waveguide Analysis* (Wiley, New York, 2001).
- <sup>21</sup>V. G. Kravets, F. Schedin, and A. N. Grigorenko, *Phys. Rev. Lett.* **101**, 087403 (2008).
- <sup>22</sup>Due to the different effective environment for the nanowires  $w$  was slightly adjusted in order to keep  $E_{p1}$  constant.